Journal of Environmental Management 240 (2019) 136–148

Contents lists available at ScienceDirect

Journal of Environmental Management

journal homepage: www.elsevier.com/locate/jenvman

Research article

Fingerprinting changes in source contribution for evaluating soil response during an exceptional rainfall in Spanish pre-pyrenees

Leticia Gaspar[a,*], Ivan Lizaga[a], William H. Blake[b], Borja Latorre[a], Laura Quijano[c], Ana Navas[a]

[a] Estación Experimental de Aula Dei, EEAD-CSIC, Avda. Montañana 1005, 50059 Zaragoza, Spain
[b] School of Geography, Earth and Environmental Sciences, University of Plymouth, Plymouth, UK
[c] Georges Lemaître Centre for Earth and Climate Research - Earth and Life Institute, Université Catholique de Louvain, Louvain-la-Neuve, Belgium

ARTICLE INFO

Keywords:
Flood event
Source provenance
Suspended sediments
FingerPro model

ABSTRACT

In the Mediterranean region, floods are expected to increase as a result of climate change and knowledge of soil erosion hot spots during exceptional rainfalls is required to support mitigation measures. This study quantifies the main sediment sources during an exceptional rainfall event in 2012 (235 mm) at the outlet of two catchments located in NE Spain. To this purpose, suspended sediments were collected during the flood event, complemented with entrapped sediments in mat taken one year after the event. We used fingerprinting methodology and applied the FingerPro unmixing model to estimate the contribution from main sources. The selected tracers clearly distinguished agricultural, rangeland, subsoil and channel banks as the four potential sources in both catchments. In the *Vandunchil* catchment, the 8 time-integrated suspended sediment samples revealed changes in source contribution during the 2-h sampling sequence. There were relatively high contributions from rangeland, agriculture and subsoil at the beginning of the sampling, representing 30, 40 and 35% of the total source contributions, respectively. Our records captured the delivery of pulses of eroded surface soil transported by runoff with direct connectivity to the stream. The sequence was followed by a sharp increase in channel bank contribution (up to 90%) in comparison to the other sources, reflecting streambank erosion and landslide occurrence, which manifested during the flood. In contrast, in the *La Reina* catchment, agricultural soils contributed the most (65%) and, together with subsoils (32%), were the main sources. These results reflect the effect of the higher connectivity and slope gradient of these cultivated fields of the *La Reina* catchment in comparison with those of the *Vandunchil* catchment.

We discuss the possibility of using different properties, such as radionuclides, geochemistry and magnetic measurements, as tracers to distinguish between potential sources during an exceptional event in upland Mediterranean catchments. Our results support the use of fingerprinting techniques to determine variations in source contribution and sediment provenance during flood events, as extreme rainfalls are main drivers of sediment mobilization and key factors in changing landscapes. This is essential in identifying vulnerable hot spots, in which early-stage interventions are needed, and for helping policy makers with management of soil and water resources.

1. Introduction

Exceptional rainfall events trigger large floods that result in severe soil and nutrient losses, important geomorphological changes. In general, during exceptional and extreme rainfall events with recurrence intervals of approximately 100 and more than 500 years, respectively, entire catchments are activated and extreme soil erosion and shallow landslides occur (Gonzalez-Hidalgo et al., 2013). The transport of enormous amounts of sediment produces severe soil and nutrient losses in some areas and sediment accumulation in others. The hydrological response of a catchment is related to the individual rainfall event and the characteristics of the catchment, such as water storage in the soil, antecedent soil moisture, land use, vegetation cover, topography and manmade infrastructures (Latron et al., 2008).

Erosion largely depends on a variety of factors, such as land use type, terrain, vegetation cover and type, inherent soil erodibility and intensity of erosive forces (e.g. Navas et al., 2008). Therefore, to control soil erosion, it is important to identify the most vulnerable areas that correspond with potential sources of mobilised sediments. Fine material in suspension is the major transport mechanism of particulate material

* Corresponding author.
E-mail addresses: leticia.gaspar.ferrer@gmail.com, lgaspar@eead.csic.es (L. Gaspar).

https://doi.org/10.1016/j.jenvman.2019.03.109
Received 27 November 2018; Received in revised form 22 March 2019; Accepted 24 March 2019
Available online 28 March 2019

in streams worldwide, typically comprising more than 90% of the annual load in alluvial streams (Meade et al., 1990). Lana-Renault et al. (2007) highlighted the importance of considering the changing locations of contributing areas of sediment during long-lasting rainstorms for understanding the complex hydrological and geomorphological behaviour of catchments. In Mediterranean environments, several studies have demonstrated that soils and vegetation cover are major factors explaining hydrological and sedimentological response caused by rainfall for different temporal and spatial scales (García-Ruiz, 2010).

Knowledge of sediment provenance is a key factor in understanding sediment transport and delivery processes (Walling, 2005). The fingerprinting technique has been successfully used to identify sediment sources in different physiographical regions around the world (Blake et al., 2012; Walling, 2013; Owens et al., 2016). The method assumes that the relative importance of potential sources can be determined by comparing several fingerprints in suspended sediment with those in potential sources. To document the suspended sediment provenance, tracer property values for the various potential sources are used in a mass balance equation to determine their relative contribution to the mixed signature in a suspended sediment sample (Collins and Walling, 2004). Different types of tracers have been used in published research including geochemistry (Laceby and Olley, 2015; Gaspar et al., 2019), radionuclides (Wallbrink et al., 1998; Collins and Walling, 2002; Gellis et al., 2017), colour (Martínez-Carreras et al., 2010a, 2010b; Pulley and Rowntree, 2016; Barthod et al., 2015), mineral magnetism (Oldfield and Wu, 2000; Rowntree et al., 2017), stable isotopes (Revel-Rolland et al., 2005) and biomarkers (Hancock and Revill, 2013).

Research on sediment characteristics, including their sources and yields, can clarify the physical and chemical properties of eroded soil, the potential nutrients and pollutants associated, the transport and redistribution mechanisms and relationships among sediment sources, sinks and outputs in rivers (Walling, 2005; Gellis and Mukundan, 2013). The use of the fingerprinting technique for tracing soil and sediment source response during rainstorms has received less attention compared with previous studies documenting deposited flood sediments (Walling, 2013), partly due to the large volumes of sample required to obtain sufficient sediment for tracing in a single, high-erosivity flood event. Several studies have examined the potential for sediment fingerprinting for recording single-erosion events using time-integrated samplers (Martínez-Carreras et al., 2010b; Gellis et al., 2017). However, although a number of studies have successfully applied various tracers to discriminate potential source materials and investigated the temporal variations of suspended sediment properties during rainfall events (Walling and Webb, 1982; Horowitz, 2008), not many studies have captured temporal variation in sediment sources in an effective way.

In this study, we aim to identify the temporal dynamics of sediment sources by unmixing suspended sediments collected during an exceptional rainfall event that occurred in 2012 in two adjacent mountain catchments in Northern Spain. Our main purposes are: i) to describe the temporal variations of suspended sediment properties during the time-integrated sampling, ii) to determine the contributions of the potential sources for the suspended sediments and capture any temporal variations, and iii) to compare the response of sediment sources to the exceptional rainfall event with records occurring during more typical events by using sediment entrapped in mats samples.

2. Study area

The study was undertaken in two adjacent catchments located in the northern part of the Ebro River Basin, Spain (Fig. 1): *Vandunchil* catchment (15.3 km^2) and *La Reina* catchment (1.8 km^2). The difference between the catchments lies largely in land use distribution, slope gradients and hydrological connectivity.

The mean annual precipitation for the study area is around 500 mm (Quijano et al., 2016). The hydrological regime is characterised by ephemeral streams and no permanent rivers. Regular stream floods result from storms in late summer and autumn, together with spring rains. The study catchments are ungauged and discharge data are not available. Geomorphological features are conditioned by sub-horizontal stratification of the lithostratigraphic units of the Uncastillo Formation.

The land use is primarily rangeland and agriculture land. Winter barley (e.g. *Hordeum vulgare*) is the main crop in the cultivated areas. Rangeland is mostly represented by scrubland, including patches of natural Mediterranean forest (e.g. *Quercus coccifera* L.) and pine afforestation areas (e.g. *Pinus halepensis* Mill.) that are restricted to the upper parts of the catchments.

The agricultural intensification increased connectivity due to enhanced overland flow favouring gullying, stream incision, formation of channel banks and severe soil erosion processes (Lizaga et al., 2019). On the other hand, the subsequent land abandonment of some areas, in addition to the natural revegetation and pine afforestation over the steep slopes during the past century, have significantly affected the runoff response, reducing the connectivity and water erosion of these areas (Lizaga et al., 2018a,b).

The *Vandunchil* catchment has 82% of its surface area (12.6 km^2) occupied by rangeland and 15% (2.3 km^2) by agriculture fields located in alluvial valley floors with gentle slopes. Rangeland occupies steep-slope areas at the headwaters, with an abundance of pine afforestation on terraces at the highest altitudes. The *La Reina* catchment is occupied by nearly 40% (0.8 km^2) agriculture lands developed on Quaternary steep glacis, while rangeland (1 km^2) occupies intermediate altitudes with less terracing. Geomorphic features related to enhanced runoff (e.g. incised stream banks) are less common in the *La Reina* catchment.

3. Material and methods

3.1. The exceptional rainfall event

In 2012, an exceptional rainfall, and subsequent flood, event occurred in the central-western Pyrenees with rainfall totalling approximately 235 mm in a two-day period, from October 19–21, 2012. The event was recorded using a tipping bucket rain gauge. The precipitation at the study site coincides with that measured at the Yesa weather station (WS) (217.2 mm, with measurements taken every 15 min) located 20-km north of the study site.

The event began at 6:45 a.m. A total of 121 mm of rain accumulated in less than 5 h, with a peak intensity of 17 mm/15 min at 9:15 a.m., 2 h before the sampling started. Stream response time, based on local observations of flooding, was estimated at 1–2 h after storms (resident personal communication). Fig. 2 shows the hydrograph for Yesa WS during the event. No human lives were lost, although the floods destroyed roads, enlarged some parts of the alluvial plain and caused landslides in the channel banks (Fig. 3).

3.2. Sampling collection

Potential source materials were sampled across the two catchments. After several field inspections, four primary sediment sources were identified: (1) agricultural topsoil, (2) rangeland topsoil, (3) bare subsoil surfaces exposed to erosion, and (4) channel banks. The number of samples obtained was approximately proportional to the area occupied by each source type (Fig. 1). Surface soils were sampled using cylindrical cores 5 cm long and 6 cm in diameter. Three samples were obtained at each site to create composite samples that were combined in the field. For the *Vandunchil* catchment, a total of 106 source samples were collected as follows: agricultural (11), rangeland (78), subsoil (7) and channel banks (10), respectively. For the *La Reina* catchment, a total of 43 source samples were obtained: agricultural (20), rangeland (14), subsoil (6) and channel banks (3).

The set of downstream sediment mixtures comprised 10 suspended sediment (SS) samples collected during the flood event, and another

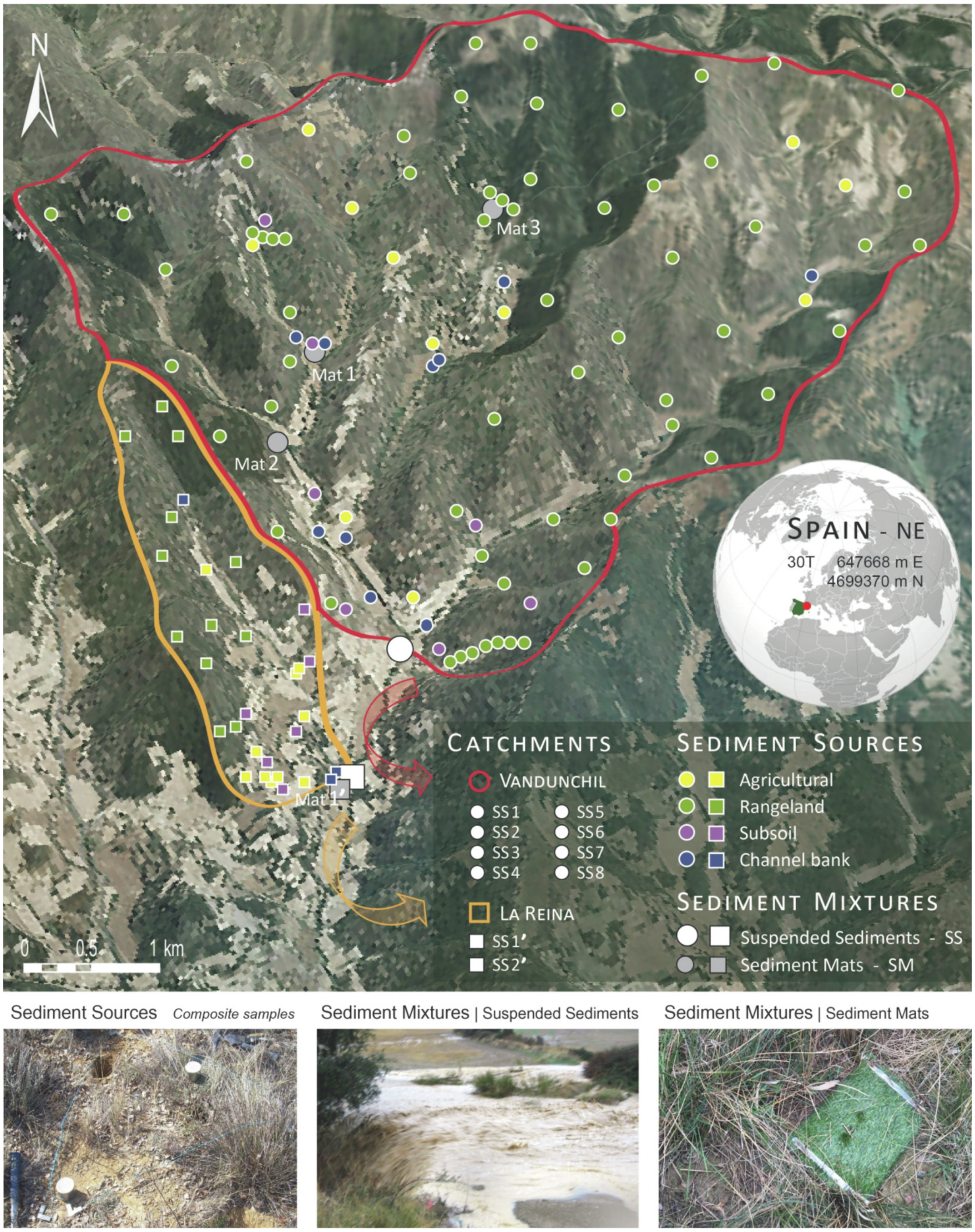

Fig. 1. *Vandunchil* and *La Reina* catchments: the orto-picture of the study area, the location of sediment sources and sediment mixtures samples, and the different sampling devices.

four sediment samples entrapped in mats (SM) collected in 2013, one year after the event. The suspended sediment samples were collected in *situ* at the outlet of both ungauged catchments (see Fig. 2). A total of 10 grab samples of stream water were collected periodically during the flood. Eight 5-L bucket samples were taken every 15 min during a 2-h period at the outlet of the *Vandunchil* catchment, and two buckets were taken at the outlet of the *La Reina* catchment. In November 2012, after the storm event, 4 sediment trap sites were installed for the two catchments: three in the *Vandunchil* catchment and one at the outlet of the *La Reina* catchment (Fig. 1). Each individual trap site consisted of three pieces of artificial turf ($25 \times 40\,cm^2$) secured to the surface with 10-cm long steel pins. A total of 12 sediment mat traps were in place for nearly one year, during which no additional exceptional events occurred.

3.3. Lab analyses

The sediment source, SS and SSC samples were air-dried, gently disaggregated, and sieved to < 63 μm. The suspended sediments (SS) were obtained by decanting the water contained in the 5-L buckets, and the suspended sediment concentration (SSC) was measured after filtering the water samples and drying the residue. Sediments entrapped in mats (SM) were extracted from the artificial turf.

Gamma emissions of ^{137}Cs, ^{226}Ra, ^{238}U, ^{232}Th, and ^{4}K were measured using a Canberra Xtra high-resolution, low-background, hyperpure germanium coaxial gamma detector (50% efficiency, 1.9-keV

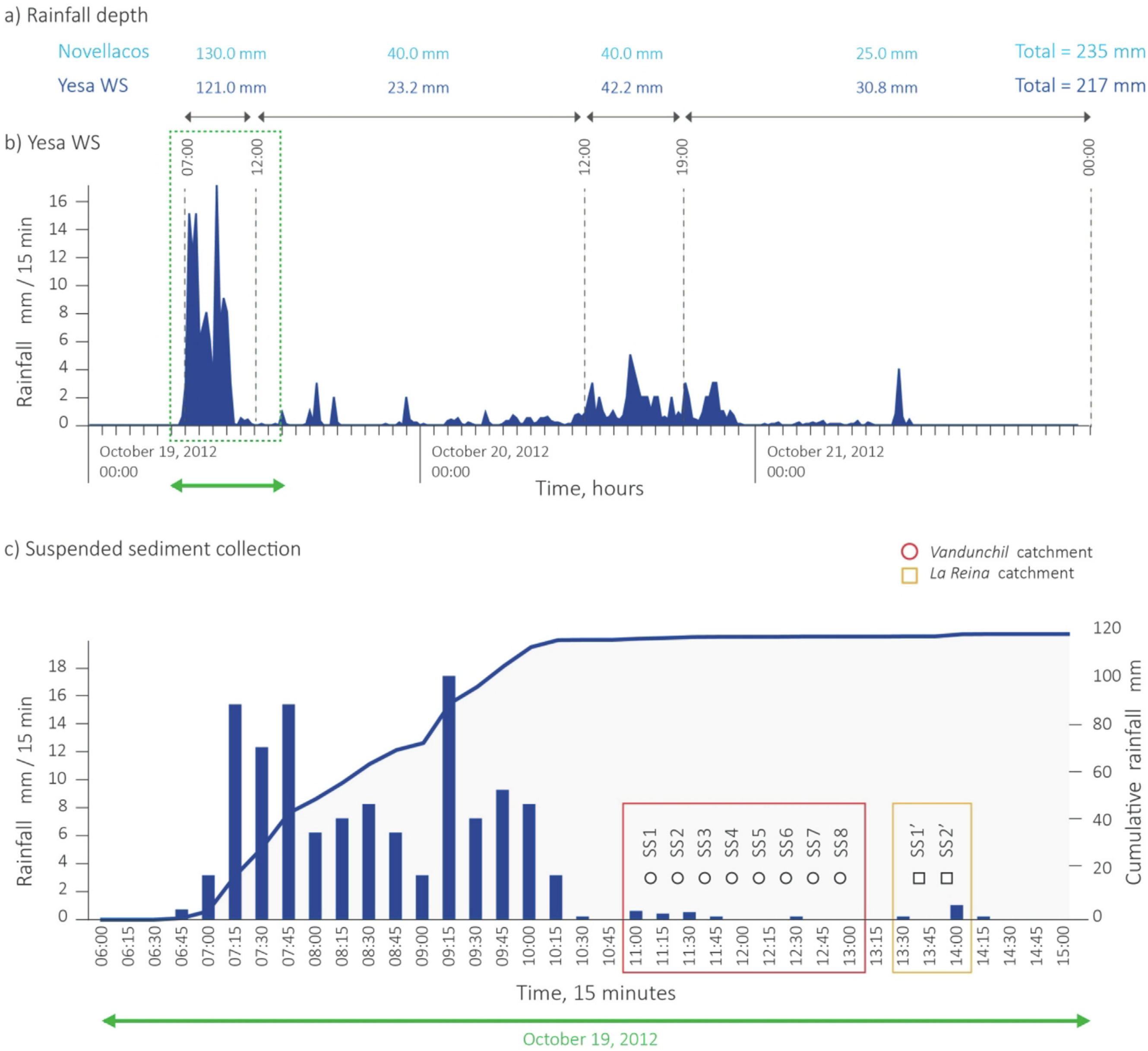

Fig. 2. Historical intraday data for the exceptional rainfall event: a) rainfall depth for Yesa WS and Novellacos site, b) 15 min hydrograph for Yesa WS, and c) detailed information for the temporal dynamic of the precipitation: peak intensity and the cumulative rainfall during the collection of suspended sediments on October 19, 2012.

resolution) (Navas et al., 2013). Count times over a 24-hr period provided an analytical precision of about ± 3–10% at a 95% level of confidence. The radionuclide activities are expressed as Bq kg^{-1} dry soil.

Elemental geochemistry was analysed by X-ray fluorescence (XRF) using a Thermo Fisher Scientific Niton XL3T 950 He GOLDD XRF analyser. Samples were packed into XRF sample cups with a 38.2-mm exposure diameter which permits the X-Ray pulse (3-mm diameter) to strike the surface of the sample. Helium was used to allow measurement of light elements, resulting in 18 elements with measurements above the detection limit (Ba, Nb, Zr, Sr, Rb, Pb, Zn, Fe, Cr, V, Ti, Ca, K, Al, P, Si, S, and Mg). Analytical quality controls recorded a very low drift of less than 1%. The mass concentration is expressed as ppm.

Low-frequency magnetic susceptibility (LF) was determined using a Bartington susceptibility meter. The content of soil organic carbon (SOC) was measured by using a dry-combustion method LECO RC-612 multiphase carbon analyser (LECO Corporation, St. Joseph, MI, USA). Particle size analyses were performed using a Coulter LS 13 320 laser diffraction particle size analyser (Beckman Coulter, Inc., 2011), after eliminating the organic matter.

3.4. Fingerprinting procedure

Standard statistical tests were used for selecting the optimal tracers (Palazón et al., 2015; Gaspar et al., 2019). The FingerPro unmixing model (Lizaga et al., 2018a) was used for estimating the contributions of sediment sources in the SS and SM samples. A total of 42 simulations were performed, evaluating three different sets of tracers: i) including P, ii) excluding P, and iii) including SOC and P.

FingerPro is a standard linear multivariate unmixing model with Monte Carlo uncertainty analysis implemented in an open-source R package within the CRAN platform (Lizaga et al., 2018a). The relative contribution of each sediment source is determined following equation 1, which satisfies the constraints of equation 2:

Fig. 3. Photos showing the impacts on the study area during and after the exceptional rainfall event.

$$\sum_{j=1}^{m} a_{i,j} \bullet \omega_j = b_i$$

$$\sum_{j=1}^{m} \omega_j = 1 \quad 0 \leq \omega_j \leq 1$$

where b_i is the tracer property i (i = 1 to n) of the sediment mixture, $a_{i,j}$ represents the tracer property i in the source type j (j = 1 to m), ω_j is the unknown relative contribution of the source type j, m represents the number of potential sediment sources and n is the number of tracer properties selected. The procedure aims to find the source proportions that conserve the mass balance, where apportionments must lie between 0 and 1 and sum 1, expressed in % (i.e. between 0 and 100, sum of 100). The source contributions estimated by the FingerPro model were expressed as the mean source contribution (pie-chart) and the frequency distribution (violin plot) of the best 100 solutions predicted by the model.

4. Results

4.1. Characteristics of the sediment sources and mixtures

The most abundant element in the sediment sources was Si, with a maximum content of 251,272 ppm. Other major elements were Ca, Al, Fe, and K (9037-251,272 ppm), followed by Mg, P, Ti, Sr and Mn (109–7528 ppm). Contents of Ba, Zr, Rb, Zn, Cr, and V ranged from 30 to 559 ppm and the trace elements Pb and Nb were below 33 ppm. The LF value ranged from 5 to 146 10^{-8} m^3 kg^{-1}, and SOC content varied from undetectable to 7%. The mass activity of ^{137}Cs ranged from 0 to 33 Bq kg^{-1}, the mean activity of ^{4}K reached 500 Bq kg^{-1}, while the mean activities of ^{226}Ra, ^{232}Th and ^{238}U were lower than 50 Bq kg^{-1}, falling within ranges of similar soils (Navas et al., 2005).

Most sediment source properties had similar ranges in both catchments, although the mean values of ^{137}Cs, LF and SOC were nearly twice in *Vandunchil* catchment than in *La Reina* catchment. For the sediment mixtures, most suspended sediment properties fell within the 5^{th}-95th percentile range of values found in the source groups.

Table 1
Mean content and standard deviation (SD) of all study properties for each source type at the Vandunchil and La Reina catchment, respectively. Properties with significance levels for discriminating between source types are shown with asterisks as potential tracers ($p < 0.05$ level, 95% confidence level).

	Vandunchil catchment								*La Reina* catchment							
	Agricultural		Rangeland		Subsoil		Channel bank		Agricultural		Rangeland		Subsoil		Channel bank	
	Mean	SD	Mean	SD	Mean	SD	Mean	SD	Mean	SD	Mean	SD	Mean	SD	Mean	SD
Si ppm	* 184,672.1	13,889.7	187,297.2	24,163.9	164,464.2	5758.8	184,900.7	13,686.9	166,985.4	7858.2	164,725.7	17,978.3	162,078.6	5995.5	172,081.8	2057.6
Ca ppm	* 148,814.0	27,746.6	128,808.9	42,756.0	171,526.3	12,313.3	150,588.0	18,706.6	170,741.5	13,007.6	166,180.4	29,243.5	177,940.8	19,717.6	169,860.6	8957.0
Al ppm	41,972.8	4064.5	40,512.3	4775.4	43,826.8	6261.8	39,392.1	2330.4	37,963.7	2965.6	35,247.4	5766.2	41,150.1	7312.3	37,396.6	3137.7
Fe ppm	* 23,997.6	2944.7	24,956.8	3971.0	23,611.5	3157.1	21,411.6	1264.2	21,097.1	1594.1	20,699.1	3231.8	21,750.8	3795.9	19,566.5	2151.8
K ppm	* 15,206.3	1484.0	15,061.2	1704.2	16,915.2	3469.0	14,243.0	1141.6	14,320.6	1186.1	13,375.2	2054.7	15,249.9	3458.0	13,288.8	1482.5
Ti ppm	* 3451.8	324.1	3400.1	387.9	3014.4	155.9	3385.2	192.1	* 3142.0	171.6	3059.9	234.4	2851.3	191.4	3168.7	97.4
Mg ppm	* 4043.5	387.6	3722.9	803.6	5053.4	1524.4	3723.1	574.4	* 3407.2	728.7	3153.5	1049.1	5219.2	1447.2	4382.4	920.4
P ppm	* 1148.4	81.6	1038.4	182.7	752.4	73.2	1112.2	98.3	* 1105.7	110.3	965.5	217.9	748.2	53.5	990.6	38.8
Ba ppm	* 313.7	38.0	279.3	38.8	370.9	64.0	340.6	29.7	* 283.9	43.2	285.8	31.5	353.0	25.6	333.9	33.1
Mn ppm	* 332.3	65.3	351.7	102.0	228.3	21.5	294.3	73.7	286.8	57.7	279.9	69.6	297.2	51.2	270.2	83.0
Sr ppm	* 351.8	73.6	317.9	130.2	545.5	187.3	422.7	81.1	* 455.9	49.2	434.1	180.2	622.6	151.6	583.7	60.1
Zr ppm	* 209.6	30.9	222.9	58.6	142.1	47.6	227.8	52.9	* 186.8	26.9	215.3	48.6	161.8	51.0	236.7	11.4
Rb ppm	* 79.5	10.5	79.3	11.4	88.8	19.8	72.5	6.3	72.1	7.5	67.7	12.7	78.2	20.1	66.3	8.7
Cr ppm	* 79.9	11.4	80.3	12.7	70.4	11.8	59.4	11.7	* 69.7	7.9	69.7	12.6	65.4	12.8	51.5	9.7
Zn ppm	* 61.7	9.8	61.2	8.9	59.4	12.1	52.3	4.1	54.8	5.0	52.9	8.6	55.0	13.0	51.4	2.8
V ppm	* 68.4	14.4	72.8	15.3	83.2	16.7	61.7	9.5	58.1	9.9	60.6	12.8	72.7	19.4	57.0	15.7
Nb ppm	11.6	1.3	11.3	1.6	10.7	0.6	11.1	0.7	10.6	0.7	10.2	1.5	10.0	0.7	10.2	1.2
Pb ppm	* 16.3	2.9	18.0	5.0	12.9	1.4	14.3	2.2	14.9	2.1	15.4	3.8	13.7	3.4	13.7	2.4
^{137}Cs Bq kg^{-1}	* 4.9	2.1	13.5	7.5	0.2	0.5	0.6	1.1	* 2.6	1.3	9.2	7.2	0.2	0.5	0.4	0.7
^{40}k Bq kg^{-1}	521.2	51.2	520.1	59.3	569.1	121.6	494.6	59.1	461.2	46.0	464.4	68.6	522.3	128.1	466.7	56.8
^{226}Ra Bq kg^{-1}	29.6	3.1	29.0	4.5	28.7	3.1	28.1	3.4	* 30.5	2.3	27.8	3.1	27.5	0.7	27.8	0.6
^{232}Th Bq kg^{-1}	34.0	3.6	34.9	4.9	34.1	4.1	33.6	2.7	30.8	2.5	31.4	3.3	31.8	5.3	31.7	3.2
^{238}U Bq kg^{-1}	44.3	6.4	44.0	10.3	45.0	9.6	40.9	10.0	36.5	10.0	37.8	4.6	38.5	4.5	35.3	3.1
LF 10^{-8} m^{3}kg^{-1}	* 59.8	21.7	62.4	32.8	10.7	5.4	19.7	8.7	* 36.3	17.0	37.5	26.2	10.9	2.5	17.8	15.4
SOC %	* 1.6	0.6	2.6	1.2	0.4	0.3	1.2	0.3	* 1.0	0.2	2.1	1.0	0.3	0.2	1.1	0.2
Clay %	17.0	2.4	14.9	3.6	13.9	4.2	13.9	1.7	12.6	2.5	13.3	2.7	11.7	3.7	10.7	2.9
Sand %	* 5.5	3.1	12.0	6.7	10.6	6.0	13.2	4.9	* 8.2	1.9	11.2	5.3	16.5	9.7	17.1	2.0

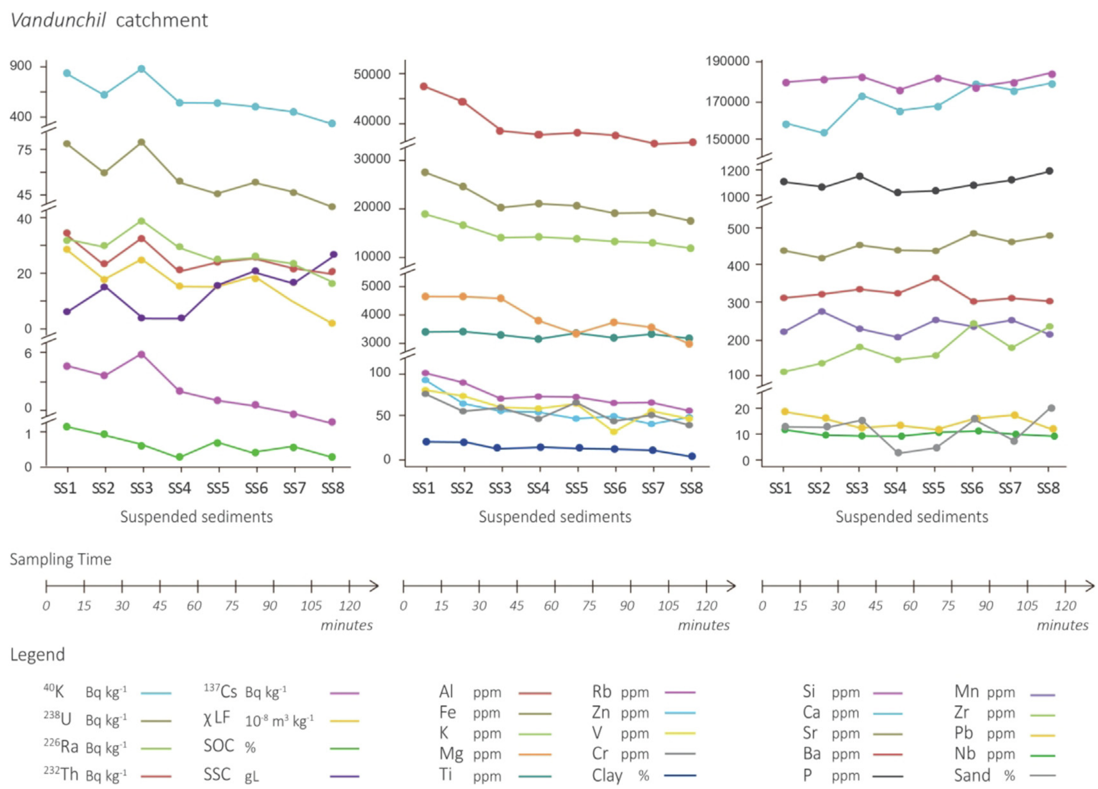

Fig. 4. The variation of the content on 27 properties in the time-integrated sequence of eight suspended sediments samples collected at *Vandunchil* catchment.

However, sediments entrapped in mats had a larger number of properties with values outside the sediment source ranges (e.g. Al, Fe, Rb, Zn, Mn, or ^{4}K) (Table 1).

During the time-integrated sampling sequence (SS1 to SS8) at the outlet of *Vandunchil* catchment, activities of ^{137}Cs, ^{4}K, ^{238}U, ^{226}Ra, ^{232}Th and LF values decreased, with the exception of a sharp increase in SS3 related to an increase in contents of Ca, Se, Zr, P and sand fraction (Fig. 4). There was also a clear decreasing trend in SOC, Al, Fe K, Mg, Rb, Zn, V, and clay content. In contrast, Si, Ca, Sr, P, Zr, and sand content increased, while Ti, Nb, and Pb varied little. The suspended sediment concentration was lower at the beginning of the sampling sequence (7.3 gL^{-1} in SS1) and progressively increased to concentrations up to 26.5 gL^{-1} in SS8 (Fig. 4).

In *La Reina* catchment, there were no differences in most properties apart from a slight increase in Mg, Se, and Ca, and a slight decrease in Ba, Mn, and Nb contents. The SSC was 19.3 and 17.9 gL^{-1} in SS1′ and SS2', respectively.

4.2. Source discrimination and tracer selection

Almost 75% and 50% of the sediment source properties were significantly different between the four source groups at the *Vandunchil* and *La Reina* catchment, respectively (Table 1). In the *Vandunchil* catchment, agricultural soils had significantly higher mean contents of P and clay fraction than the other sources. Rangeland soils were characterised by the highest means of ^{137}Cs, SOC, Si, Fe, Cr and Pb, but had significantly lower contents of Ca, Sr, and Ba than in subsoils. Subsoils recorded the highest contents of Ca, K, Mg, Sr, Ba, Rb, and V, and the lowest of P, SOC, Mn, and Zr contents. Channel banks had a significantly lower mean of Fe, Ti, Cr, Zn, and clay contents than the other sources. Like subsoil and agricultural soils, channel banks had also low SOC and high Zr contents. Similarly to subsoils, channel banks had low LF and ^{137}Cs activity (Table 1).

In *La Reina* catchment, agricultural soils had significantly higher mean P and ^{226}Ra contents than the other sources, while the highest ^{137}Cs and SOC were in rangeland soils. Subsoils registered significantly higher means of Mg, Sr, and sand content but lower mean of SOC, P, LF, and Ti than the other sources. Channel banks were enriched in Ti and Zr, similar to rangeland soils, and in Ba similar to subsoils. However, mean Cr content was significantly lower than in the other sources (Table 1).

Different properties, in number and type, were selected as optimum composite fingerprint tracers (Table 2). For the *Vandunchil* catchment, the first seven suspended sediment samples (SS1 to SS7) had the same 9 optimum fingerprints. In most cases, ^{137}Cs and LF were the selected tracers, followed by Fe (except for SS8 and SM), Ba and Cr (except for SM1), P (except for SM2), and Ca (except for SM3). Tracers like Ti and V were also selected for most sediment mixtures except for SM1 and SM3. For the *La Reina* catchment, fewer properties met the selection criteria, but similar to the *Vandunchil* catchment, ^{137}Cs, Ba, Ti, and P were the selected tracers, along with Mg. In addition, tracers like Zr and Sr were used for SS1′ and SS2'.

Both catchments showed a clear discrimination between the four sources (Fig. 5). Discriminant function analysis (DFA) plots show a clear distinction between subsoils and channel banks. Differences were less

Table 2
Optimum fingerprint tracers obtained with the assessed statistical test (range test, Kruskal Wallis test and DFA test) for each of suspended sediments (SS) and sediment mats (SM) collected at the two study catchments.

Sediment mixtures	n	Tracers
Vandunchil catchment		
SS 1, SS 2, SS 3, SS 4, SS 5, SS 6, SS 7	9	^{137}Cs, LF, Ba, Fe, Cr, Ti, Ca, V, P
SS 8	9	^{137}Cs, LF, Ba, Zn, Cr, Ti, Ca, V, P
SM 1	7	^{137}Cs, LF, Ba, Cr, Ti, Ca, V
SM 2	6	^{137}Cs, LF, Ca, V, Sr, P
SM 3	6	^{137}Cs, LF, Ba, Cr, Zr, P
La Reina catchment		
SS 1′, SS 2′	7	^{137}Cs, Ba, Ti, Zr, Sr, Mg, P
SM 1′	5	^{137}Cs, Ba, Ti, Mg, P

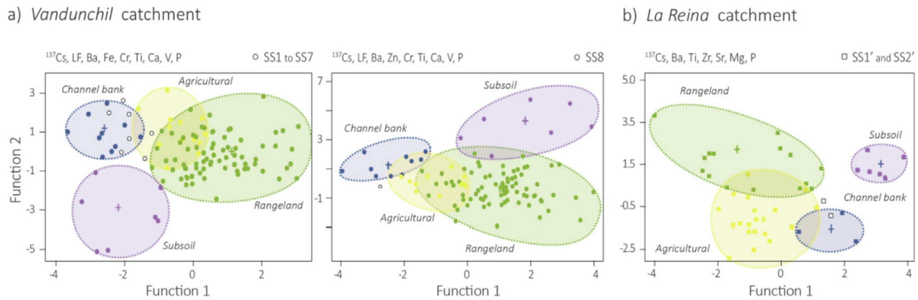

Fig. 5. Two-dimensional scatterplots of the first and second discriminant functions from stepwise discriminant function analysis (DFA) using the optimum tracer selected for a) *Vandunchil* catchment and b) *La Reina* catchment. Ellipsoid encompasses 95% of group range.

clear between agricultural and rangeland soils because overlapping occurred for some samples, especially in the *Vandunchil* catchment. Despite that, for both catchments, DFA step-wise produced a set of tracers that allowed correct classification of 100% of the channel bank samples, 98% of subsoils and around 90% of agricultural and rangeland soils.

4.3. Source contributions for the suspended sediments

In the *Vandunchil* catchment, the source provenance for the time-integrated sampling varied greatly from SS1 to SS3, with little variations observed from SS4 to SS8. The contribution from agricultural and rangeland soils decreased exponentially during the sampling sequence. A similar decreasing pattern, but less evident, occurred for the subsoil contributions (Fig. 6). However, apportions from channel bank had a clear exponential increase from SS1 to SS8.

The dispersion of the source contributions varied from low SD values (0.7%) up to 19% (Table 3). Agricultural and rangeland soils yielded the highest SDs in SS1 to SS3, but the lowest in SS4 to SS8. The SDs for subsoil were consistently around 7%, while channel bank saw a low SD in SS1 and high SDs in SS2 to SS8. These results changed when P was excluded as an optimum tracer, resulting in increased uncertainty for all sources. The inclusion of SOC did not affect uncertainty estimates (Table 3).

The frequency distributions of the estimated subsoil contributions showed narrow, symmetrical and unimodal distributions. Agricultural and rangeland contributions for SS1 showed symmetrical frequency distributions, while for SS6 to SS8 the symmetrical distributions where less clear. A multimodal pattern was observed in SS3 for the agricultural soils (Fig. 6).

In the *La Reina* catchment, similar source contributions were estimated for SS1′ and SS2’. The agricultural soils contributed the most, more than doubling the subsoils apportions. The rangeland soils and channel bank together, contributed less than 2% and 7% for SS1′ and SS2′, respectively. The range of solutions varied little (SD from 1.7 to 9%), especially for SS1' with SD values lower than 6.5%. The frequency distribution for agricultural soils and subsoil was symmetrical and unimodal, whereas for rangeland soils and channel bank was less symmetric but narrow enough (Fig. 7).

4.4. Source contributions for the sediment entrapped in mats

Different source contributions, depending on the location of the mats, were observed in the *Vandunchil* catchment. Sediment mat SM1, located upstream of SM2, recorded channel bank as the main apportion. In contrast, SM2 showed that subsoil was the main contributing source, with around 20% sourced from channel bank. The dispersion of the results was higher in SM2 than in SM1, but with SD lower than 7% for most estimated source contributions, apart from channel bank and subsoil in SM2 (Fig. 6). After several trials, it was not possible to unmix SM3.

At the outlet of the *La Reina* catchment, SM1′ showed similar source contributions to the suspended sediment samples SS1′ and SS2’ (Fig. 7). Agricultural soil was the predominant source and contributed almost three times more than subsoil. However, the contribution of rangeland soils and channel bank in SM1′ was at least twice as much as the contribution recorded for SS1′ and SS2’ (Table 4). Despite similarities between the results obtained for suspended sediments and the sediment entrapped in mats, SM1' had wider and less symmetric frequency distributions than those of the suspended sediments samples (Fig. 7).

5. Discussion

5.1. Optimum composite fingerprints

The capability of ^{137}Cs in discriminating between sediment sources is a result of large differences between ^{137}Cs activities in the soil sources. The high ^{137}Cs mass activity in rangeland reflects the effect of vegetation cover's protection of the soil surface while the low content in agricultural soils is due to dilution by mixing during tillage (Gaspar et al., 2013; Gaspar and Navas, 2013). For the other sources, the absence of the radionuclide is consistent with erosion of topsoil layers in subsoil, while verticality of channel banks prevents ^{137}Cs tagging with the bank materials. Large contents of Sr, Ca, Ba, Mg, V, and K in subsoil are related to the carbonatic characteristics of parent materials, which concentrate these elements (Navas and Machín, 2002), but also to the high capacity of clay minerals to absorb these elements (Kabata-Pendias and Pendias, 2001; Navas and Lindhorfer, 2003). The low Ti content in subsoil might reflect the effects of weathering. As Ti minerals are very stable, the loss of some clay-size layered silicates might increase the amount of Ti in the upper soil horizons (Kabata-Pendias and Pendias, 2001). Therefore, the better-developed and undisturbed soils, such as in rangeland sources, could be more enriched in Ti than eroded areas, represented by subsoil.

Differences in Fe between sources are likely related to oxides and hydroxides that are more abundant in better-developed soils, which predominate in rangeland. The highest SOC contents and LF values in rangeland are in agreement with significant positive correlations between SOC and magnetic properties, also reported by Quijano et al. (2014) and confirm the potential for using magnetic properties in tracking soil degradation in this environment. Mineral magnetism was also successfully applied as a single tracer for suspended sediments samples collected through consecutive storm events in South Africa (Rowntree et al., 2017).

Though controversies about the use of nutrients as tracers persist, largely due to their potentially non-conservative behaviour during transport (Withers and Jarvie, 2008; Koiter et al., 2013), P is used to investigate the contribution of sediment related to agricultural activities (Walling et al., 2008) and can track cropland or pasture erosion (Ben Slimane et al., 2013; Lamba et al., 2015). We used P and SOC because of the short transport length, the brief duration of the sampling sequence, and the rapid flood that prevented soil storage (Blake et al.,

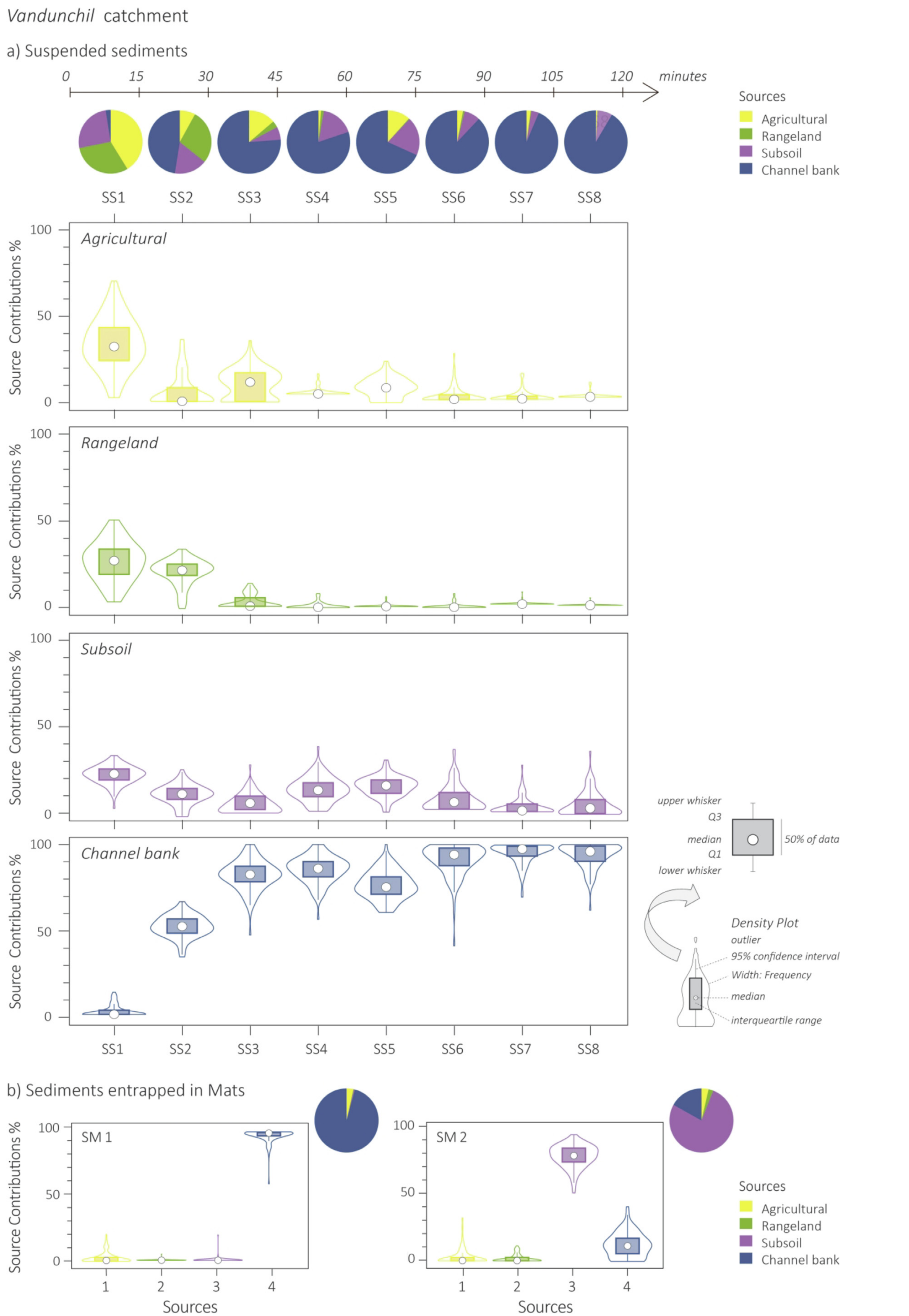

(caption on next page)

Fig. 6. Estimated source contribution and frequency distribution for the sediments mixtures collected at *Vandunchil* catchment: a) for the time-integrated sequence of eight suspended sediments (SS1 to SS8) and b) for sediment entrapped in mats (SM1 and SM2).

2006).

Both P and SOC are of value for distinguishing between sources. The benefits of including them as tracers relate to providing less variability to the source contributions (Tables 3 and 4, see GOF values). The significantly higher content of P in agricultural soils than in the other sources supports its likely origin from fertilisers. In addition, alkaline soils in the study area, with low SOC and secondary accumulation of carbonates, may play an important role in the equilibria between the particulate and dissolved P fractions through the possible presence in our soils of the carbonate-fluorapatite mineral (Ca_5 (PO_4, CO_3)) (OH, F)) (Vidal, 1988).

The high values of Ca, P, and sand content that peak in SS3, in coincidence with low clay content, denote a common mineral origin. The increase of P and Ca from SS4 to SS8, in which we estimated a clear predominance of channel bank soil contribution also supports a mineral origin for P. Further, the enriched Ca content in subsoil and channel banks, in line with the presence of Ca in different forms, increases the soil retention capacity of P, which binds readily to Ca. Other soil characteristics, like SOC, pH, and texture, also influence the availability of P in soil (i.e. finer textures have a greater capacity to replace P than coarser textures). Furthermore, sediment deposition in channel beds, and subsequent remobilisation, exert an important influence on the transport and fate of particulate P in catchments (Owens and Walling, 2002). Jarvie et al. (2005) observed that P stored in sediments can be re-released as dissolved P after reduction, though such releases would make small changes to the overall P signature at our scale. Further, soil erosion processes have also been shown to affect the partitioning of P between dissolved vs. Particulate forms during runoff events (Huisman et al., 2013).

Our results are in agreement with the developing idea that tracer selection should be also supported by knowledge of hydrological, geomorphological, and geochemical processes controlling tracer behaviour. Other studies also support the selection of appropriate soil properties as fingerprinting tracers not solely on the basis of statistical procedures (e.g., Smith et al., 2018).

5.2. Source contribution variations during the flood event

A varied response to the rainfall event and runoff was clearly detected between the two adjacent study catchments, reflecting, among others, differences in land use, physiography and connectivity in the catchments. To this respect, in the *La Reina* catchment, agricultural soils are the major source of suspended sediments because of its higher connectivity and steeper slopes of cultivated fields in contrast with the *Vandunchil* catchment.

In the *Vandunchil* catchment at the beginning of the extreme flood, agricultural and rangeland topsoils were primary sources, along with subsoil. However, as the event progressed, channel bank become the main source. The agricultural contribution in the early stages of the flood is indicated by higher SOC content at the beginning of the sampling sequence, rather than later. Although runoff transported rangeland soil particles at the initiation of the event, its signal declined later.

Table 3
Source contributions (%) estimated with FingerPro unmixing model for the eight suspended sediments (SS) and the sediment mats (SM) collected at the *Vandunchil* catchment. Three different simulations for each sediment mixture are listed: i) using the optimum tracers, ii) excluding P as a tracer, or iii) adding SOM as an additional tracer.

Vandunchil		GOF	Agricultural		Rangeland		Subsoil		Chanel bank	
Sediment mixtures		%	mean	SD	mean	SD	mean	SD	mean	SD
SS 1	i	78.7	41.2	19.4	30.6	14.9	25.7	6.8	2.5	4.4
	ii	74.8	22.0	18.6	33.3	14.3	44.4	8.7	0.2	1.2
	iii	79.1	39.8	19.9	0.2	1.2	28.6	6.9	4.0	5.8
SS 2	i	81.7	8.0	12.2	27.7	9.8	16.8	7.5	47.5	8.2
	ii	74.3	10.2	14.9	23.1	11.2	39.1	10.3	27.6	11.2
	iii	81.7	8.4	13.0	24.1	9.2	19.8	7.4	47.7	9.3
SS 3	i	76.7	13.8	11.3	3.4	5.2	6.6	6.6	76.2	11.3
	ii	72.9	10.3	10.4	2.9	4.6	24.6	10.2	62.2	12.7
	iii	77.4	11.3	9.6	1.9	3.4	7.8	5.7	79.0	10.7
SS 4	i	75.4	1.3	3.2	1.4	2.5	17.1	9.2	80.2	10.0
	ii	67.8	2.3	5.3	0.8	1.9	36.3	13.5	60.6	14.0
	iii	76.0	1.2	4.1	0.4	1.0	18.3	7.7	80.1	9.6
SS 5	i	84.8	11.6	7.4	0.4	1.3	19.7	7.5	68.2	10.6
	ii	78.1	10.4	9.7	0.3	1.2	38.3	9.7	51.0	13.2
	iii	86.0	9.7	7.1	0.1	0.8	20.7	6.1	69.4	9.7
SS 6	i	64.0	3.0	5.8	0.8	2.1	8.2	9.8	88.0	12.2
	ii	63.2	1.6	4.1	0.9	2.2	4.9	7.7	92.6	9.1
	iii	65.8	2.2	5.8	0.2	0.2	7.7	8.4	89.9	12.0
SS 7	i	75.6	2.1	4.1	0.3	1.1	3.9	6.3	93.6	7.7
	ii	70.2	2.6	5.4	0.2	0.6	20.5	12.0	76.8	13.0
	iii	76.8	1.5	3.4	0.1	0.2	3.6	5.1	94.8	6.5
SS 8	i	67.3	0.7	2.0	0.3	0.7	7.5	9.1	91.5	9.3
	ii	69.5	0.6	2.3	0.2	0.3	11.6	9.7	87.6	10.3
	iii	68.9	0.8	2.6	0.1	0.1	6.9	7.9	92.2	8.8
SM 1	i	68.1	3.4	5.6	0.3	0.7	0.5	2.7	95.7	7.1
	ii	68.1	3.4	5.6	0.3	0.7	0.5	2.7	95.7	7.1
	iii	67.2	2.4	6.0	0.2	0.2	1.9	5.5	95.5	9.1
SM 2	i	80.6	3.6	7.4	2.4	4.0	77.1	11.7	16.9	12.8
	ii	79.3	0.8	2.8	3.1	4.1	82.3	18.5	13.8	19.0
	iii	90.1	0.7	3.2	4.2	4.4	54.8	9.8	40.3	12.4
SM 3	i	–	–	–	–	–	–	–	–	–
	ii	–	–	–	–	–	–	–	–	–
	iii	–	–	–	–	–	–	–	–	–

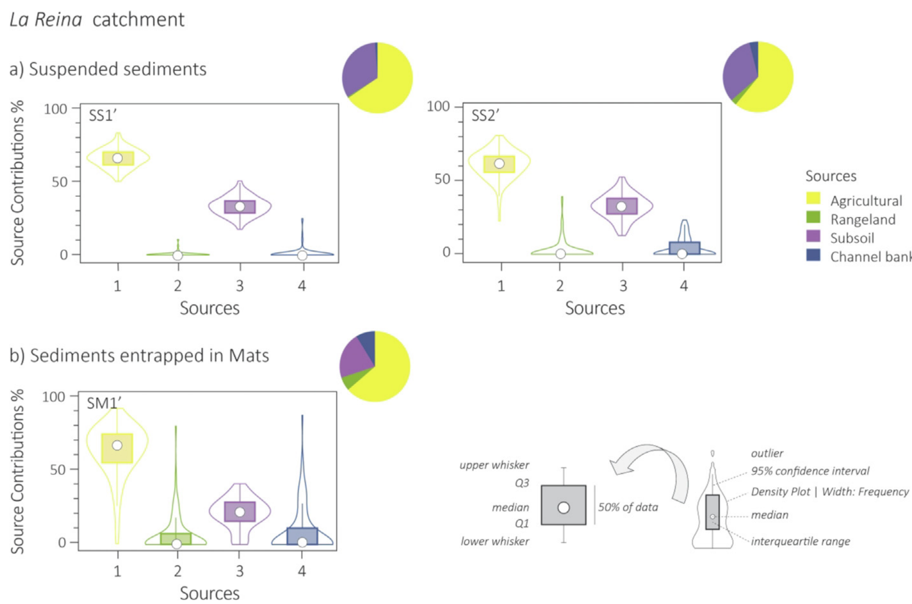

Fig. 7. Estimated source contribution and frequency distribution for the sediments mixtures collected at *La Reina* catchment: a) for two suspended sediments (SS1′ and SS2′) and b) for sediment entrapped in mats (SM1′).

Table 4
Source contributions (%) estimated with FingerPro unmixing model for the two suspended sediments (SS) and the sediment mat (SM) collected at the *La Reina* catchment. Three different simulations for each sediment mixture are listed: i) using the optimum tracers, ii) excluding P as a tracer, or iii) adding SOM as an additional tracer.

La Reina		GOF	Agricultural		Rangeland		Subsoil		Chanel bank	
Sediment mixtures		%	mean	SD	mean	SD	mean	SD	mean	SD
SS 1′	i	83.6	65.4	6.5	0.6	1.7	32.9	6.4	1.1	3.9
	ii	81.3	66.8	10.0	0.7	2.9	31.0	7.2	1.5	5.3
	iii	83.2	65.5	6.7	0.2	0.7	32.8	6.5	1.5	4.0
SS 2′	i	78.1	60.9	9.6	2.7	6.8	32.4	8.2	4.0	6.5
	ii	78.4	64.3	14.8	1.8	7.6	29.8	9.4	4.1	9.1
	iii	78.1	60.9	9.6	2.7	6.8	32.4	8.2	4.0	6.5
SM 1′	i	76.6	63.7	17.4	6.2	12.2	21.4	10.3	8.7	15.8
	ii	72.5	59.2	21.4	10.7	17.1	24.3	12.3	5.7	14.4
	iii	69.2	50.1	19.5	1.2	3.6	30.1	11.6	18.5	25.3

A reason could be the topography of the catchment with clear sub-horizontal stratification, along with the abundance of linear elements due to terracing for pine afforestation that retains the mobilised sediments. In addition, vegetation cover seems efficient in protecting soil and preventing further sediment mobilization, even under this exceptional disturbance.

In contrast, evidence of streambank erosion from SS4 to SS8 is supported by the predominant contribution of channel bank and the highest SSC values. The importance of streambank erosion is further evidenced by changes in the channel section observed after the exceptional rainfall, which produced streambanks failure that resulted in a widening of the channel section. Palmer et al. (2014) also recorded high streambank erosion when precipitation was 26% above normal. Factors affecting bank erosion under high flooding conditions are related to the hydraulic forces exerted on the stream, which create unstable conditions that result in bank failure and mass wasting (Wynn, 2006).

The suspended sediment dynamic and the temporal variability of the relative source contributions are linked to several factors, including the distribution of land uses, connectivity, and changes in the stream channel (i.e. failure of loose streambanks) (Fig. 2). Other authors also point to sediment connectivity, in addition to modifications in contributing areas (Evrard et al., 2010), hydraulic boundary and antecedent soil moisture conditions.

This study has captured the signal of rangeland soils that, under regular rainfall, is difficult to obtain because these soils are protected by vegetation cover and terracing. The field observations during and after the storm event allowed us to identify intense rilling and new gully formation in agricultural and rangeland soils that support the estimated source apportions. Our results suggest that the new connectivity created during the event worked efficiently to transport sediment to the stream. This indicates that connectivity between the headwaters and our sampling locations was unobstructed and was able to effectively transport sediments throughout the stream channel. In earlier work, Koiter et al. (2013) similarly highlight the importance of the sampling location and the need to incorporate the catchment connectivity to understand how efficiently the sediment is transported from the headwaters to the outlet. In the *La Reina* catchment, comparable results obtained for the suspended sediments (SS1′, SS2′) and for the sediment mat (SM1') confirm that source contributions were similar during the exceptional rainfall and during periods of regular precipitation. The high connectivity of the catchment and the predominance of agricultural soils on Quaternary steep glacis is the reason why these soils are the major source of sediments.

Under regular functioning of ephemeral streams, the main difference of an exceptional event is that rangeland soils and, to lesser extent, agricultural soils and subsoils are less well connected with the drainage system because of terracing, vegetation strips, furrows, and other linear

elements of the landscape that protect soil from erosion. Fryirs (2013) identified three types of blockages (buffers, barriers, and blankets), indicating that their spatial arrangement will exert an influence on the connectivity and, subsequently, on the pattern of sediment transport and storage (Hooke and Mant, 2000; Kuo and Brierley, 2013). However, for intense rainfalls, the connectivity of agricultural and rangelands increases, leading to high sediment loads in the streams. Only unusual high-magnitude events like this event are able to produce enough surface runoff to connect the hydrological system with the sources of sediment. After soil particles are disaggregated by runoff, due to fluctuations in runoff transport capacity, the particles can be temporarily stored inside the fields, preventing them from reaching the streams. On the other hand, the large discharges that reach the streams increase channel erosivity and cause landslides thus increasing the signal of channel bank.

Our results during this exceptional event, along with previous research on connectivity in the study area (Lizaga et al., 2019), allow us to better understand the variation of source apportions. Due to human impact on Mediterranean landscapes, these uplands agroecosystems streams produce infilling of valley floors that are later incised. The landscape evolution has led to the presence of a mosaic of land uses and different surface covers that influence the connectivity of sediment sources to the river network. We can conclude that the change in dominant source during the sampling sequence in the *Vandunchil* catchment is due to changes in sediment storage and connectivity, reflecting a transition in the dominant erosion processes from topsoil to streambank erosion.

6. Conclusions

This study provided a detailed record of temporal variations in relative source contributions to the total sediment flux through time during an exceptional rainfall event. Our results demonstrated the potential for using ^{137}Cs, along with stable elements and magnetic properties as effective tracers. In addition, our study has proven the efficiency of the FingerPro model in determining quantitative source contributions to capture a change in dominant source. The different characteristics of the study catchments, in terms of distribution of land uses and structural connectivity of the landscape, played a key role in controlling sediment availability and the prominence of the contributing source. The rainfall event activated the entire *Vandunchil* catchment, transporting sediment from sources that, during regular flood events, remain disconnected, and allowed for the sediment to surpass the linear elements that typically interrupt the connectivity of the landscape. The predominant contributions of agricultural, rangeland and subsoil sources, in addition to the lowest concentration of suspended sediments and the highest SOC contents, support topsoil erosion occurring at the beginning of the exceptional event, while later peaks of SSC and high contributions of channel bank suggest a shift to a predominance of streambank erosion.

One of the main findings from our study is the temporal variability in source provenance recorded during the 2-h sampling sequence at the outlet of the *Vandunchil* catchment, which demonstrates the need to generate high spatial and temporal resolution source apportionments, especially during storm-events.

Sediment fingerprinting approaches offer important insights into the nature of erosion and transport processes that operate in Mediterranean upland catchments supporting that exceptional events are main drivers of the process dynamic leading to landscape changes.

Acknowledgements

This research was funded by the project (CGL 2014-52986-R). We thanks Dr Javier Machín for the valued rainfall records and sampling data obtained during the exceptional rainfall event.

References

Barthod, L.R., Liu, K., Lobb, D.A., Owens, P.N., Martínez-Carreras, N., Koiter, A.J., Petticrew, E.L., McCullough, G.K., Liu, C., Gaspar, L., 2015. Selecting color-based tracers and classifying sediment sources in the assessment of sediment dynamics using sediment source fingerprinting. J. Environ. Qual. 44 (5), 1605–1616.
Blake, W.H., Walsh, R.P.D., Sayer, A.M., Bidin, K., 2006. Quantifying fine-sediment sources in primary and selectively logged rainforest catchments using geochemical tracers. Water Air Soil Pollut. Focus 6 (5–6), 615–623.
Blake, W.H., Ficken, K.J., Taylor, P., Russell, M.A., Walling, D.E., 2012. Tracing crop-specific sediment sources in agricultural catchments. Geomorphology 139–140, 322–329.
Ben Slimane, A., Raclot, D., Evrard, O., Sanaa, M., Lefèvre, I., Ahmadi, M., Tounsi, M., Rumpel, C., Ben Mammou, A., Le Bissonnais, Y., 2013. Fingerprinting sediment sources in the outlet reservoir of a hilly cultivated catchment in Tunisia. J. Soils Sediments 13, 801–815.
Collins, A.L., Walling, D.E., 2002. Selecting fingerprint properties for discriminating potential suspended sediment sources in river basins. J. Hydrol. 261, 218–244.
Collins, A.L., Walling, D.E., 2004. Documenting catchment suspended sediment sources: problems, approaches and prospects. Prog. Phys. Geogr. 28, 159–196.
Evrard, O., Nord, G., Cerdan, O., Souchère, V., Le Bissonnais, Y., Bonté, P., 2010. Modelling the impact of land use change and rainfall seasonality on sediment export from an agricultural catchment of the northwestern Environ. Eur. Loess Belt. Agric. Ecosyst. 138 (1–2), 83–94.
Fryirs, K., 2013. Disconnectivity in catchment sediment cascades, a fresh look at the sediment delivery problem. Earth Surf. Process. Landforms 38, 30–46.
García-Ruiz, J.M., 2010. The effects of land uses on soil erosion in Spain. A review. Catena 81 (1), 1–11.
Gaspar, L., Navas, A., 2013. Vertical and lateral distributions of ^{137}Cs in cultivated and uncultivated soils on Mediterranean hillslopes. Geoderma 207–208, 131–143.
Gaspar, L., Navas, A., Walling, D.E., Machín, J., Gómez Arozamena, J., 2013. Using ^{137}Cs and $^{210}Pb_{ex}$ to assess soil redistribution on slopes at different temporal scales. Catena 102, 46–54.
Gaspar, L., Blake, W.H., Smith, H.G., Lizaga, I., Navas, A., 2019. Testing the sensitivity of a multivariate mixing model using geochemical fingerprints with artificial mixtures. Geoderma 337, 498–510.
Gellis, A.C., Mukundan, R., 2013. Watershed sediment source identification: tools, approaches and case studies. J. Soils Sediments 13, 1655–1657.
Gellis, A.C., Fuller, C.C., Van Metre, P.C., 2017. Sources and ages of fine-grained sediment to streams using fallout radionuclides in the Midwestern United States. J. Environ. Manag. 194, 73–85.
Gonzalez-Hidalgo, J.C., Batalla, R.J., Cerda, A., 2013. Catchment size and contribution of the largest daily events to suspended sediment load on a continental scale. Catena 102, 40–45.
Hancock, G.J., Revill, A.T., 2013. Erosion source discrimination in a rural Australian catchment using compound-specific isotope analysis (CSIA). Hydrol. Process. 27, 923–932.
Hooke, J.M., Mant, J.M., 2000. Geomorphological impacts of a flood event on ephemeral channels in SE Spain. Geomorphology 34, 163–180.
Horowitz, A.J., 2008. Determining annual suspended sediment and sediment-associated trace element and nutrient fluxes. Sci. Total Environ. 400 (1–3), 315–343.
Huisman, N.L.H., Karthikeyan, K.G., Lamba, J., Thompson, A.M., Peaslee, G., 2013. Quantification of seasonal sediment and phosphorus transport dynamics in an agricultural watershed using radiometric fingerprinting techniques. J. Soils Sediments 13 (10), 1724–1734.
Jarvie, H.P., Jürgens, M.D., Williams, R.J., Neal, C., Davies, J.J.L., Barrett, C., White, J., 2005. Role of river bed sediments as sources and sinks of phosphorus across two major eutrophic UK river basins: the Hampshire Avon and Herefordshire Wye. J. Hydrol. 304 (1), 51–74.
Kabata-Pendias, A., Pendias, H., 2001. Trace Elements in Soils and Plants. CRC, Boca Raton, pp. 315.
Koiter, A.J., Owens, P.N., Petticrew, E.L., Lobb, D.A., 2013. The behavioural characteristics of sediment properties and their implications for sediment fingerprinting as an approach for identifying sediment sources in river basins. Earth Sci. Rev. 125, 24–42.
Kuo, C.W., Brierley, G.J., 2013. The influence of landscape configuration upon patterns of sediment storage in a highly connected river system. Geomorphology 180–181, 255–266.
Laceby, J.P., Olley, J., 2015. An examination of geochemical modelling approaches to tracing sediment sources incorporating distribution mixing and elemental correlations. Hydrol. Process. 29 (6), 1669–1685.
Lamba, J., Karthikeyan, K.G., Thompson, A.M., 2015. Using radiometric fingerprinting and phosphorus to elucidate sediment transport dynamics in an agricultural watershed. Hydrol. Process. 29, 2681–2693.
Lana-Renault, N., Regues, D., Marti-Bono, C., Begueria, S., Latron, J., Nadal, E., et al., 2007. Temporal variability in the relationships between precipitation, discharge and suspended sediment concentration in a small Mediterranean mountain catchment. Nord. Hydrol 38, 139–150.
Latron, J., Soler, M., Llorens, P., Gallart, F., 2008. Spatial and temporal variability of the hydrological response in a small Mediterranean research catchment (Vallcebre, Eastern Pyrenees). Hydrol. Process. 22, 775–787.
Lizaga, I., Latorre, B., Gaspar, L., Navas, A., 2018a. fingerPro: an R Package for Sediment Source Tracing. https://CRAN.R-project.org/package=fingerPro. https://doi.org/10.5281/zenodo.1402029.
Lizaga, I., Quijano, L., Palazón, L., Gaspar, L., Navas, A., 2018b. Enhancing connectivity index to assess the effects of land use changes in a Mediterranean catchment. Land

Degrad. Dev. 29, 663–675.
Lizaga, I., Quijano, L., Gaspar, L., Ramos, M.C., Navas, A., 2019. Linking land use changes to variation in soil properties in a Mediterranean mountain agroecosystem. Catena 172, 516–527.
Martínez-Carreras, N., Udelhoven, T., Krein, A., Gallart, F., Iffly, J.F., Ziebel, J., Hoffmann, L., Pfister, L., Walling, D.E., 2010a. The use of sediment colour measured by diffuse reflectance spectrometry to determine sediment sources: application to the Attert River catchment (Luxembourg). J. Hydrol. 382, 49–63.
Martínez-Carreras, N.F., Krein, A., Udelhoven, T., Gallart, F., Iffly, J.F., Hoffmann, L., Pfister, L., Walling, D.E., 2010b. A rapid spectral-reflectance-based fingerprinting approach for documenting suspended sediment sources during storm runoff events. J. Soils Sediments 10 (3), 400–413.
Meade, R.H., Yuzyk, T.R., Day, T.J., 1990. Movement and storage of sediment in rivers of the United States and Canada. In: The Geology of North America, vols. 0–1. pp. 225–280 Surface Water Hydrology. The Geological Society of America.
Navas, A., Machín, J., 2002. Spatial distribution of heavy metals and arsenic in soils of Aragon (northeast Spain): controlling factors and environmental implications. Appl. Geochem. 17, 961–973.
Navas, A., Lindhorfer, H., 2003. Geochemical speciation of heavy metals in semiarid soils of the central Ebro Valley (Spain). Environ. Int. 29 (1), 61–68.
Navas, A., Soto, J., Machín, J., 2005. Mobility of natural radionuclides and selected major and trace elements along a soil toposequence in the central Spanish Pyrenees. Soil Sci. 170 (9), 743–757.
Navas, A., Machín, J., Beguería, S., López-Vicente, M., Gaspar, L., 2008. Soil properties and physiographic factors controlling the natural vegetation re-growth in a disturbed catchment of the Central Spanish Pyrenees. Agrofor. Syst. 72, 173–185.
Navas, A., López-Vicente, M., Gaspar, L., Machín, J., 2013. Assessing soil redistribution in a complex karst catchment using fallout ^{137}Cs and GIS. Geomorphology 196, 231–241.
Oldfield, F., Wu, R., 2000. The magnetic properties of the recent sediments of Brothers Water, N W England. J. Paleolimnol. 2 (2), 165–174.
Owens, P.N., Walling, D.E., 2002. The phosphorus content of fluvial sediment in rural and industrialized river basins. Water Res. 36, 685–701.
Owens, P.N., Blake, W.H., Gaspar, L., Gateuille, D., Koiter, A.J., Lobb, D.A., Petticrew, E.L., Raiffarth, D., Smith, H.G., Woodward, J.C., 2016. Fingerprinting and tracing the sources of soils and sediments: earth and ocean science, geoarchaeological, forensic, and human health applications. Earth Sci. Rev. 162, 1–23.
Palazón, L., Latorre, B., Gaspar, L., Blake, W.H., Smith, H.G., Navas, A., 2015. Comparing catchment sediment fingerprinting procedures using an auto-evaluation approach with virtual sample mixtures. Sci. Total Environ. 532, 456–466.
Palmer, J.A., Schilling, K.E., Isenhart, T.M., Schultz, R.C., Tomer, M.D., 2014. Streambank erosion rates and loads within a single watershed: bridging the gap between temporal and spatial scales. Geomorphology 209, 66–78.
Pulley, S., Rowntree, K., 2016. The use of an ordinary colour scanner to fingerprint sediment sources in the South African Karoo. J. Environ. Manag. 165, 253–262.
Quijano, L., Chaparro, M.A.E., Marié, D.C., Gaspar, L., Navas, A., 2014. Relevant magnetic and soil parameters as potential indicators of soil conservation status of Mediterranean agroecosystems. Geophys. J. Int. 198, 1805–1817.
Quijano, L., Gaspar, L., Navas, A., 2016. Spatial patterns of SOC, SON, ^{137}Cs and soil properties as affected by redistribution processes in a Mediterranean cultivated field (Central Ebro Basin). Soil Tillage Res. 155, 318–328.
Revel-Rolland, M., Arnaud, F., Chapron, E., Desmet, M., Givelet, N., Alibert, C., McCulloch, M., 2005. Sr and Nd isotopes as tracers of clastic sources in Lake Le Bourget sediment (NW Alps, France) during the Little Ice Age: palaeohydrology implications. Chem. Geol. 224, 183–200.
Rowntree, K.M., van der Waal, B.W., Pulley, S., 2017. Magnetic susceptibility as a simple tracer for fluvial sediment source ascription during storm events. J. Environ. Manag. 194, 54–62.
Smith, H.G., Karam, D.S., Lennard, A.T., 2018. Evaluating tracer selection for catchment sediment fingerprinting. J. Soils Sediments 18, 3005–3019.
Vidal, M., 1988. Contenido y dinámica del fósforo en el sedimento de praderas de fanerógamas marinas. Oecol. Aquat. 9, 41–59.
Wallbrink, P.J., Murray, A.S., Olley, J.M., Olive, L.J., 1998. Determining sources andtransit times of suspended sediment in the Murrumbidgee River, New South Wales, Australia, using fallout ^{137}Cs and ^{210}Pb. Water Resour. Res. 34, 879–887.
Walling, D.E., 2005. Tracing suspended sediment sources in catchments and river systems. Sci. Total Environ. 344, 159–184.
Walling, D.E., 2013. The evolution of sediment source fingerprinting investigations in fluvial systems. J. Soils Sediments 1310, 1658e–1675.
Walling, D.E., Webb, B.W., 1982. Sediment Availability and the Prediction of Storm-Period Sediment yields.Recent Developments in the Explanation and Prediction of Erosion and Sediment Yield, vol. 137. IAHS Publication, pp. 327–337.
Walling, D.E., Collins, A.L., Stroud, R.W., 2008. Tracing suspended sediment and particulate phosphorus sources in catchments. J. Hydrol. 350, 274–289.
Withers, P.J.A., Jarvie, H.P., 2008. Delivery and cycling of phosphorus in rivers: a review. Sci. Total Environ. 400, 379–395.
Wynn, T., 2006. Streambank retreat-A primer: watershed update, January–March 2006. Am. Water Resour. Assoc. Hydrol. Watershed Manag. Tech.Committee 4 (1), 1–14 February 15, 2014.